MR-Tidal: A System for Efficient Respiration Tracking in Clinically Constrictive Environments

Samuel Wilcox
Department of Biomedical Engineering
Georgia Institute of Technology
Atlanta, USA
swilcox33@gatech.edu

Yue Chen
Department of Biomedical Engineering
Georgia Institute of Technology
Atlanta, USA
yue.chen@bme.gatech.edu

Alexander T. Adams
College of Computing
Georgia Institute of Technology
Atlanta, USA
aadams322@gatech.edu

***Abstract*—Accurate respiratory tracking is essential for targeting dynamic organs during oncology procedures, yet current solutions struggle in constrictive clinical environments like MRI and radiotherapy suites. We propose a novel, low-profile respiratory tracking device using only a nasal cannula and remote flow sensing to overcome these limitations. The system was evaluated in two experiments: a flow distance study confirming signal fidelity across 20 meters of tubing (Pearson correlation = 0.9938 ± 0.0021), and a flow mapping study showing that the cannula captured 1% of total respiratory flow and, when scaled, could show the full respiratory cycle. The device was also tested in the MRI suite. These results demonstrate the feasibility of a simple, non-invasive solution for accurate respiratory monitoring in constrained clinical settings.**

***Index Terms*—Sensing, Gas sensing, flow sensing, organ tracking, respiration gated imaging, MRI, radiotherapy, tidal volume**

I. Introduction

Across any medical intervention, accuracy is paramount to treatment success. This objective is straightforward in static target locations, but in dynamic organs, various natural motions, mainly respiratory motion, complicate procedural delivery [1]. Targeting these dynamic organs is especially important in oncology. Cancers of abdominal organs and the lungs are highly dynamic and account for 23.5% of the US cancer burden and 38.3% of cancer mortality [2].

Given that many cancer treatments like radiotherapy and ablations are highly destructive, accurate targeting of the tumor location is important [3], [4]. This is why radiotherapy commercially pioneered respiratory tracking in systems like the CyberKnife and Radixact in order to predict tumor location [5]. These original methods of tracking were highly invasive, utilizing the implantation of fiducials and tracking via 4DCT scanning [6]. However, this additional risk and procedure time led to the development of less invasive approaches including body-mounted sensors and camera-based systems.

Camera-based approaches typically use fiducials mounted to the abdomen and track their displacement to estimate the respiratory cycle [7], [8]. Body-mounting sensors are more diverse in application and include an inertial measurement unit (IMU) [9], pneumatic padding [10], and strain sensing [11]. While these systems have their merits, they are not suited for constrictive environments that are becoming more prevalent in cancer treatments. The magnetic resonance imaging (MRI) suite [12] and proton and photon therapy centers [13] specifically have achieved significant growth and saturation.

Body-mounted solutions have two major issues in these environments. First, traditional electronic components are heavily damaged either through the magnetism of the MRI [14] or the bombardment from radiation [15]. Second, they often need to work in conjunction with other devices that obscure the body. In MRI-guided interventions, unobstructed access to the abdomen is required either by the clinician or a robotic system delivering a needle in order to maintain simple surgical workflows [16]. In proton and photon therapy, patients are in a body-fitting brace across the entire torso to control their position, not allowing for body-mounted devices [17]. Camera-based approaches have similar limitations. In both application areas it is complicated to get a clear view of the abdomen, either due to the ergonomics of the closed-bore of the MRI scanner or due to the aforementioned brace over the torso. Additionally, these systems are subject to interference from other motions not directly related to respiration and can be inaccurate. This can be solved by directly measuring respiration using tools like nasal cannulas as has been explored in sleep tracking [18], [19], though these applications remain untested in constrained clinical environments.

Given the limitations of these existing techniques, there is a need for a low-profile and accurate method of respiratory tracking that is compatible with the constrictive environments pervasive in oncology. In this paper, we propose a novel respiratory tracking system based only through a nasal cannula that provides direct respiratory tracking for all patients. This solution removes electronics from the harmful environments without body-mounted hardware or the need for line-of-sight, making it a viable solution for oncology workflows.

II. Methods and Materials

A. Device Design

The goal of the device was to develop a straightforward sensing package that integrates seamlessly with any imaging suite and allows for reliable and accessible troubleshooting (Fig. 1A). To capture respiratory signals, we selected a standard nasal cannula (HCS4514, Medline, USA) for its comfort,

This material is based upon work supported by the National Science Foundation Graduate Research Fellowship Program under Grant No. DGE-2039655. Any opinions, findings, and conclusions or recommendations expressed in this material are those of the author(s) and do not necessarily reflect the views of the National Science Foundation.

compatibility, and abundance in most clinical settings. In the interest of simplicity and minimal hardware, we opted to use a single flow sensor (SFM3400-33-AW, Sensirion, Switzerland), functionally similar to those used in traditional spirometry. The nasal cannula connects to the flow sensor via pneumatic tubing of customizable length to accommodate various setups. All components are disposable, supporting low-cost and sanitary use across multiple patients. The flow sensor outputs are read by a microcontroller. For experimental validation, we used the Arduino Due (Arduino, Italy) due to its ability to support multiple flow sensor inputs simultaneously. For clinical deployment, we also tested the Arduino Nano 33 IoT (Arduino, Italy), which provides a smaller form factor and wireless capability at lower cost.

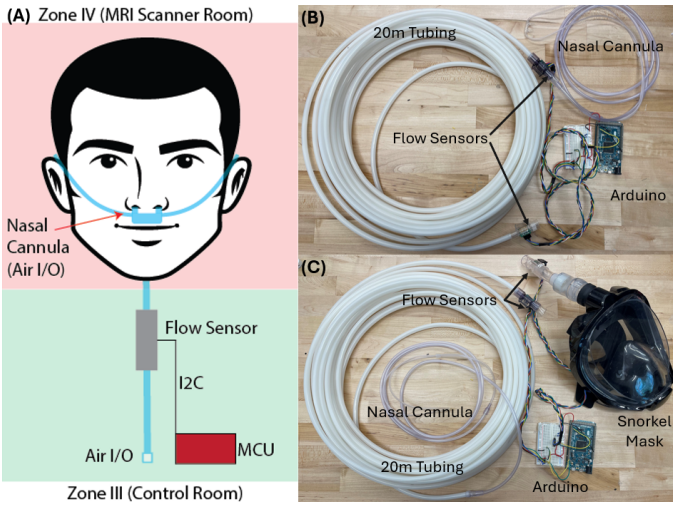

Fig. 1. (A) A systems level model of the proposed device showcasing the simplicity and workflow. (B) Setup for the flow distance experiment showing the positioning of each flow sensor used at each end of the tubing. (C) Setup of the flow mapping experiment with snorkel and attached flow sensor shown.

B. Flow Distance Experimental Setup

To move the electronics away from the harmful environments in the chosen design, the respiration measured by the flow sensor must travel through long pneumatic tubing. This distance could degrade the quality of signal we are getting due to pressure loss or turbulent flow in the tubing. An experiment was designed to determine if the measured flow was significantly impacted over a long distance. A second flow sensor, identical to the one in the device was connected to the Arduino. One flow sensor was positioned at the end of the nasal cannula line and the other was connected after 20 meters of 0.275" inner-diameter pneumatic tubing (Fig. 1B). Feedback from clinicians who work with MRI pointed to 10 meters being sufficient to pass from the patient through the wave guide and to a sensing unit in the control room, so it was doubled to definitively show the effect of pneumatic tubing.

C. Flow Mapping Experimental Design

The goal of this experiment was to evaluate the tidal volume of a patient's respiratory cycle. After validating that flow can be accurately measured over long tubing distances, it became necessary to assess how the cannula captures the inhaled and exhaled air during respiration as a ratio of the entire cycle. To accomplish this, a full-face snorkel mask was used to enclose the participant's nose and mouth, ensuring that all inhaled and exhaled air could be captured and measured. The mask was chosen due to its tight seal and single-channel design for airflow, which minimizes leakage and simplifies flow measurement. A flow sensor (SFM3300-AW, Sensirion, Switzerland) with a larger internal diameter was affixed to the outlet of the mask to reduce airflow resistance and allow unobstructed measurement of total respiratory volume (Fig. 1C). Simultaneously, the designed device measured flow through a nasal cannula, which was inserted into the mask. Care was taken to route the nasal cannula tubing without crimps to allow for unimpeded flow. This experiment was also conducted with a commodity spirometer (Go Direct Spirometer, Vernier, USA) on the masks output, replacing the flow sensor. Note the mask was only used in this experiment to capture the full breathing cycle and no changes to that cycle were observed.

III. Results

A. Flow Distance Results

Utilizing the setup described in subsection II-B, 18 trials were carried out, each measuring respiration for 30 seconds. These trials included breathing from two different persons in different positions commonly used in imaging: supine, prone, and standing. For each person and position, 3 trials were carried to make up a robust data set. To assess the relationship between the two flow sensors, the data was mean centered. A normalized cross-correlation was then computed to estimate any temporal lag between the signals, and the maximum correlation value identified the sample offset corresponding to the best alignment. Following synchronization, the Pearson correlation coefficient was calculated between the raw values of both sensors to quantify their relationship (Fig. 2).

The measured Pearson coefficient across all 18 trials was an average of 0.99384 ± 0.00214, demonstrating a consistent and strong relationship between the two signals. This means that there is not an observed change in flow across 20 meters of tubing and any length up to that can be used reliably in clinical settings. Additionally, the time-delay measured between the two sensors was 0 seconds across all trials. Given our sampling rate was 50 Hz, any potential delay is under our sampling threshold and less than 20 ms.

B. Flow Mapping Results

Upon completion of the distance experimentation, the approach described in II-C was used across 10 trials. Two different persons' breathing patterns were recorded over 5 one minute trials to produce the data which was used for analysis. The breathing data from all individual trials was combined into a single dataset. The first assessment was to determine the total measure of air throughout the respiratory cycle and the ratio captured by the cannula. Given the two sensors captured the full respiratory cycle, the measured flow in liters per minute

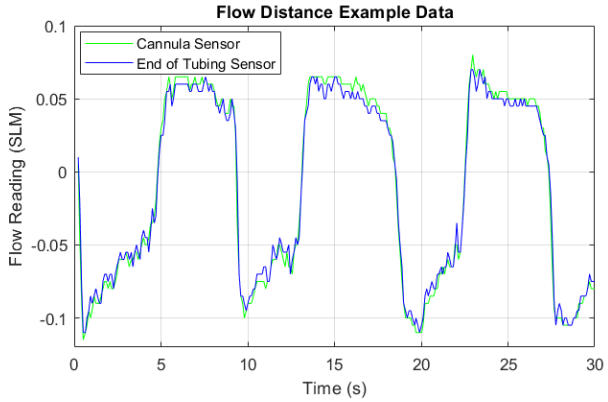

Fig. 2. Example data showing flow data from both sensors of one of the supine breathing trials. The green represents signal from the sensor at the end of the cannula line and the blue represents signal from the sensor at the end of the 20 meters of tubing.

(SLM) of each was combined to get the total flow. The percent contribution of the nasal cannula was then measured as a percentage of the total flow at every data point. The measured average percent contribution of the cannula to total flow was 1.0059%.

To assess whether this small portion of flow captured by the nasal cannula could reliably represent the overall respiratory signal, the cannula signal was scaled by a factor of 100 and compared to the full respiratory signal. This comparison was performed using three regression models, linear, fine tree, and rational quadratic gaussian process, to evaluate the ability of the cannula-derived signal to reconstruct the full breathing pattern across the respiratory cycle (Table I). The best performance was observed with the quadratic regression model, which was attempted after noticing the shape of the prediction plot of the linear regression (Fig. 3).

TABLE I
MASK FLOW-CANNULA RESULTS PER MODEL

Model	RMSE	MSE	R^2	MAE
Tree	0.030916	0.000956	0.99092	0.025098
Linear	0.055566	0.003087	0.97068	0.042731
Quadratic	**0.030628**	**0.0009381**	**0.99109**	**0.025086**

These results suggest that despite capturing only 1% of the total flow, the nasal cannula signal contains sufficient temporal and morphological information to accurately represent the overall respiratory waveform across the breathing cycle.

Upon verification that the cannula can accurately capture and model the total respiratory cycle, a spirometer, the gold standard in respiratory volume measurement, was used to track normal respiration and measured tidal volume of 0.31 L with a respiration rate of 11.5 and minute volume 3.59 L/Min. This is consistent with the same measures calculated from the flow mapping experiment as displayed in Table III.

We then repeated the flow mapping experiment with the spirometer replacing the masks flow sensor. The results, as seen in Table II, were comparable to the flow sensor results

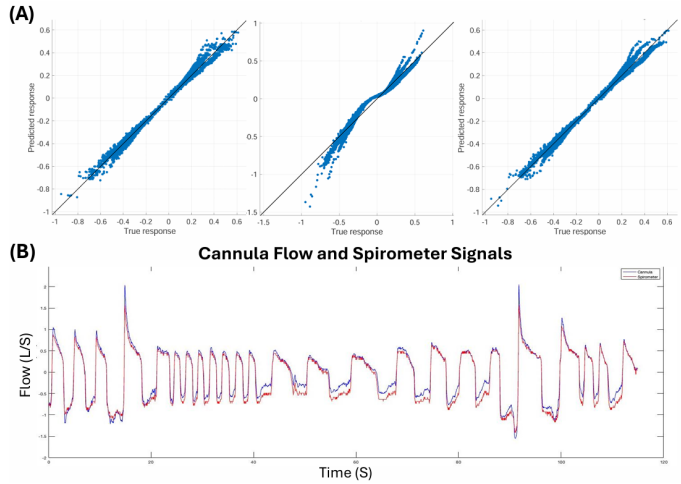

Fig. 3. (A) Prediction plots from left to right for the tree, linear, and quadratic models that were tested. (B) Predicted values versus true values over time for the quadratic regression model.

TABLE II
SPIROMETER MASK - CANNULA QUADRATIC REGRESSION RESULTS

RMSE	MSE	R^2	MAE	Peak-to-Peak	Error
0.0376	0.0014	0.9958	0.0287	2.9785 L	0.97%

in Table I. Given the performance of the cannula approach and its similarity to the current gold standard of respiratory tracking, there is significant promise for its implementation.

TABLE III
TIDAL VOLUME ANALYSIS PER TRIAL (CANNULA) (MASK) (TOTAL)

Trial	Tidal Volume *(mL) (L) (L)*	Respiration Rate *BPM*	Minute Volume *mL/min L/min L/min*
P1-1	(0.25) (0.22) (0.22)	14.5	(3.62) (3.21) (3.21)
P1-2	(0.26) (0.24) (0.24)	12.5	(3.27) (3.02) (3.02)
P1-3	(0.30) (0.28) (0.28)	14.5	(4.39) (4.00) (4.00)
P1-4	(0.38) (0.32) (0.32)	11.5	(4.41) (3.70) (3.70)
P1-5	(0.32) (0.29) (0.29)	11.5	(3.71) (3.33) (3.33)
P2-1	(0.42) (0.40) (0.40)	15.5	(6.48) (6.15) (6.16)
P2-2	(0.42) (0.38) (0.38)	16.5	(6.90) (6.33) (6.34)
P2-3	(0.34) (0.34) (0.34)	15.5	(5.20) (5.24) (5.25)
P2-4	(0.39) (0.38) (0.38)	15.5	(6.04) (5.84) (5.85)
P2-5	(0.38) (0.36) (0.36)	14.5	(5.51) (5.22) (5.22)

C. MRI Validation

Following benchtop validation of our device's ability to map nasal airflow to total tidal volume, it was essential to evaluate its performance in the MRI environment for which it was designed. The MRI suite was selected due to its more complex workflow integration compared to typical therapy centers. To assess real-world performance, the device was tested on one subject in a Siemens 3.0 Tesla Prisma FIT MRI scanner under Emory IRB 00019157. For comparison, two additional respiration sensors commonly used in the clinical setting were also deployed: a respiration transducer (TSD221-MRI, BIOPAC Systems, Inc., USA) and an integrated scanner sensor (Siemens Healthineers, Germany). Unlike our device,

the other sensors were body-mounted and exhibited a much lower signal-to-noise ratio due to interference from non-respiratory body motion. In contrast, our device maintained the same performance as in the benchtop setting and required less than five minutes to set up, demonstrating its suitability for use in constrained clinical environments such as the MRI suite. The signal-to-noise ratio for three separate recordings on the MRI were 4.56, 9.85, and 12.1 compared to 4.9, 9.0, and 8.7 in the lab experiments, indicating that there was negligible (if any) additional noise introduced from the MRI.

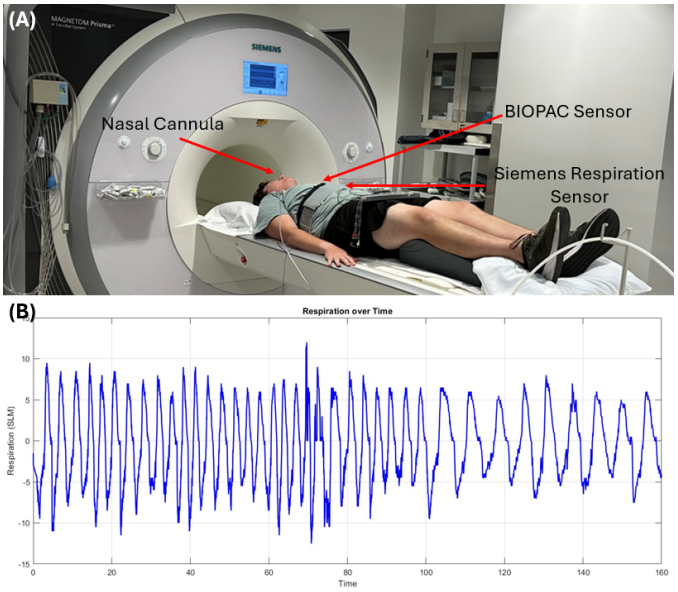

Fig. 4. (A) An example of the setup in the MRI scanner, including the three used respiration sensor. (B) Example of tracked respiration during a 160 second interval in the scanner (SNR = 5.76 dB).

IV. Discussion

The goal of this device is to provide a low-profile, accessible, and accurate method for mapping respiration in clinically constrictive environments. The system demonstrated effective respiratory monitoring in both benchtop settings and more complex environments, such as MRI scanners. Notably, despite capturing only 1% of total airflow, the nasal cannula produced results comparable to the gold standard of spirometry. Moreover, because the device captures respiration directly rather than relying on body-mounted sensors, it is less susceptible to motion artifacts from non-respiratory movement, which is an advantage particularly relevant in the MRI suite.

While these findings are encouraging, several limitations remain. First, the system depends on nasal breathing, which may not be natural or feasible for all patients. This limitation could be addressed by replacing the cannula with a respiratory mask. Second, further investigation is needed to assess whether synchronized respiratory data can predict tumor motion, which could improve the precision of treatment delivery. These limitations highlight important directions for future work, including expanded testing and clinical validation. In conclusion, this device presents a promising, low-profile solution for accurate respiratory tracking across clinical settings.

References

[1] S. Wilcox, Z. Huang, J. Shah, X. Yang, and Y. Chen, "Respiration-induced organ motion compensation: A review," *Annals of Biomedical Engineering*, vol. 53, no. 2, pp. 271–283, 2025.

[2] R. L. Siegel, A. N. Giaquinto, and A. Jemal, "Cancer statistics, 2024," *CA: a cancer journal for clinicians*, vol. 74, no. 1, pp. 12–49, 2024.

[3] H. Keum, E. Cevik, J. Kim, Y. M. Demirlenk, D. Atar, G. Saini, R. A. Sheth, A. R. Deipolyi, and R. Oklu, "Tissue ablation: Applications and perspectives," *Advanced Materials*, vol. 36, no. 32, p. 2310856, 2024.

[4] P. G. Prasanna, K. Rawojc, C. Guha, J. C. Buchsbaum, J. U. Miszczyk, and C. N. Coleman, "Normal tissue injury induced by photon and proton therapies: Gaps and opportunities," *International Journal of Radiation Oncology* Biology* Physics*, vol. 110, no. 5, pp. 1325–1340, 2021.

[5] B. T. Collins, S. Vahdat, K. Erickson, S. P. Collins, S. Suy, X. Yu, Y. Zhang, D. Subramaniam, C. A. Reichner, I. Sarikaya *et al.*, "Radical cyberknife radiosurgery with tumor tracking: an effective treatment for inoperable small peripheral stage i non-small cell lung cancer," *Journal of hematology & oncology*, vol. 2, pp. 1–9, 2009.

[6] B. T. Collins, K. Erickson, C. A. Reichner, S. P. Collins, G. J. Gagnon, S. Dieterich, D. A. McRae, Y. Zhang, S. Yousefi, E. Levy *et al.*, "Radical stereotactic radiosurgery with real-time tumor motion tracking in the treatment of small peripheral lung tumors," *Radiation Oncology*, 2007.

[7] C. N. Cho, J. H. Seo, H. R. Kim, H. Jung, and K. G. Kim, "Vision-based variable impedance control with oscillation observer for respiratory motion compensation during robotic needle insertion: a preliminary test," *The International Journal of Medical Robotics and Computer Assisted Surgery*, vol. 11, no. 4, pp. 502–511, 2015.

[8] L. Zheng, H. Wu, L. Yang, Y. Lao, Q. Lin, and R. Yang, "A novel respiratory follow-up robotic system for thoracic-abdominal puncture," *IEEE Transactions on Industrial Electronics*, vol. 68, no. 3, 2020.

[9] M. Abayazid, T. Kato, S. G. Silverman, and N. Hata, "Using needle orientation sensing as surrogate signal for respiratory motion estimation in percutaneous interventions," *International journal of computer assisted radiology and surgery*, vol. 13, pp. 125–133, 2018.

[10] A. L. Gunderman, M. Musa, B. O. Gunderman, F. Banovac, K. Cleary, X. Yang, and Y. Chen, "Autonomous respiratory motion compensated robot for ct-guided abdominal radiofrequency ablations," *IEEE Transactions on Medical Robotics and Bionics*, vol. 5, pp. 206–217, 2023.

[11] M. Chu, T. Nguyen, V. Pandey, Y. Zhou, H. N. Pham, R. Bar-Yoseph, S. Radom-Aizik, R. Jain, D. M. Cooper, and M. Khine, "Respiration rate and volume measurements using wearable strain sensors," *NPJ digital medicine*, vol. 2, no. 1, p. 8, 2019.

[12] A. B. Rosenkrantz, L. C. Cerdas, D. R. Hughes, M. P. Recht, S. J. Nass, and H. Hricak, "National trends in oncologic diagnostic imaging," *Journal of the American College of Radiology*, vol. 17, 2020.

[13] W. F. Hartsell, C. B. Simone II, D. Godes, J. Maggiore, M. P. Mehta, S. J. Frank, J. M. Metz, and J. I. Choi, "Temporal evolution and diagnostic diversification of patients receiving proton therapy in the united states: A ten-year trend analysis (2012 to 2021) from the national association for proton therapy," *International Journal of Radiation Oncology* Biology* Physics*, vol. 119, no. 4, pp. 1069–1077, 2024.

[14] J. Kihlberg, B. Hansson, A. Hall, A. Tisell, and P. Lundberg, "Magnetic resonance imaging incidents are severely underreported: a finding in a multicentre interview survey," *European radiology*, vol. 32, 2022.

[15] M. Mirzaei, P. Rowshanfarzad, S. Gill, M. A. Ebert, and J. Dass, "Risk of cardiac implantable device malfunction in cancer patients receiving proton therapy: an overview," *Frontiers in Oncology*, vol. 13, 2023.

[16] S. Wilcox, S. Sengupta, C. Huang, J. Tokuda, A. Lu, D. Woodrum, and Y. Chen, "Development of a low-profile, piezoelectric robot for mr-guided abdominal needle interventions," *Annals of Biomedical Engineering*, vol. 53, no. 7, pp. 1638–1650, 2025.

[17] A. J. Wroe, D. A. Bush, R. W. Schulte, and J. D. Slater, "Clinical immobilization techniques for proton therapy," *Technology in Cancer Research & Treatment*, vol. 14, no. 1, pp. 71–79, 2015.

[18] R. Thurnheer, X. Xie, and K. E. Bloch, "Accuracy of nasal cannula pressure recordings for assessment of ventilation during sleep," *American journal of respiratory and critical care medicine*, vol. 164, 2001.

[19] J.-J. Hosselet, R. G. Norman, I. Ayappa, and D. M. Rapoport, "Detection of flow limitation with a nasal cannula/pressure transducer system," *American journal of respiratory and critical care medicine*, vol. 157, no. 5, pp. 1461–1467, 1998.